






## Study of End-Effector of (2DOF) Five-Bar Robot Positioning: Accuracy, Modeling and Simulation

Mohammed Mousa Al-azzawi<sup>1\*</sup>, Hasan Shakir Majdi<sup>2</sup>, Atheer Raheem Abdullah<sup>1</sup>

<sup>1</sup> Department of Refrigeration and Air Conditioning, Al-Rafidain University College, Baghdad 10001, Iraq

<sup>2</sup> Department of Chemical Engineering and Petroleum Industries, Al-Mustaqbal University College, Hillah 51001, Iraq

Corresponding Author Email: [Mohammed.azzawi55@gmail.com](mailto:Mohammed.azzawi55@gmail.com)

Copyright: ©2024 The authors. This article is published by IETA and is licensed under the CC BY 4.0 license (<http://creativecommons.org/licenses/by/4.0/>).

<https://doi.org/10.18280/jesa.570203>

### ABSTRACT

**Received:** 22 September 2023

**Revised:** 2 February 2024

**Accepted:** 14 March 2024

**Available online:** 28 April 2024

#### Keywords:

*five-bar planar robot, gripping positioning accuracy, Matlab-Simulink*

Closed-chain parallel robots play a vital role in industrial applications especially in automating production processes using end-effector robots. Understanding and optimizing these systems is essential to optimize manufacturing processes, enhance accuracy and reduce errors. This study delves into an automated system consisting of five planar joints, including kinematics, dynamics, path planning, electric motors, driving systems, and the use of algorithms to enhance location accuracy through automatic control using Matlab-Simulink. Realistic computer simulations were also used to verify the validity of these methods within the studied system. The research also aims to develop this field by developing advanced control algorithms for motors, and also proposing simplified automatic control algorithms. It also aims to enhance position accuracy, taking into account evaluation metrics such as repeatability and positional error, all through discussing potential real-world applications or practical implications of the proposed control algorithms. and improved accuracy, such that this work contributes to the continued development of closed-chain parallel robots and their practical applications in industrial environments.

## 1. INTRODUCTION

Robotic systems are considered one of the most complex engineering systems because they include many interconnected systems that work simultaneously and in an integrated manner so that the robot can perform its work as required. The robot can be viewed as an overlay of a mechanical system represented by arms, joints, and other mechanical components to connect its physical parts to an electrical system. Electronic is represented by motors (mostly motors), driving circuits, sensors, control devices, and microprocessors. The integrated robot system also requires an in-depth and detailed study that includes all stages of its operation and work [1].

The study of any robot system of its various types can be discussed according to ordered steps that begin with studying the kinematics of the robot system, including the study of forward kinematics and the study of reverse kinematics, where through kinematics we can know and determine the generalized coordinates of the robot according to the degree of freedom of the robot. We do not overlook the importance of studying the movement of active joints and connections (i.e. those directly connected to the motors) because they transmit movement to the rest of the robot's parts. In addition, through inverse kinematics, the generalized coordinates according to which joints must move to transfer the coordinates of the robot's end effector to new coordinates in space [2].

Later, the dynamic study of the robot is carried out based on the Newton-Euler equations or the Euler-Lagrange equations (most often). Moreover, the main goal of the dynamic study is to determine the torque required from the motors during the operation of the robot and thus the specifications of the motors required for the robot. In the next step, through path planning, the generalized coordinates of the end effector are determined over time by studying the path planning of the robot's end effector according to inverse kinematics [3, 4]. Path planning plays a crucial role in automatic control by serving as reference signals for the control system to achieve.

Mentioning the sensors and drive systems of the motors in the control system is important, due to their importance in determining precise positions. Therefore, it is necessary to explain how these components, such as feedback sensors and motor drive systems, are specifically integrated into the control system of the five-bar planar robot and their impact on enhancing the accuracy and efficiency of position control [5].

#### Acronyms

$l_0$ : (horizontal distance of the joint 4/1 from the origin) (m)

$l_1$ : length of link No1 (m)

$l_2$ : length of link No2 (m)

$l_3$ : length of link No3 (m)

$l_4$ : length of link No4 (m)

$l_{c1}$ : the distance from the joint 1 to the center of mass of the link 1 (m)

$l_{c2}$ : the distance from the joint 1 to the center of mass of the link 2 (m)

$l_{c3}$ : the distance from the joint 1 to the center of mass of the link 3 (m)

$l_{c4}$ : the distance from the joint 1 to the center of mass of the link 4 (m)

$X$ : x coordinate of the end-effector (m)

$Y$ : y coordinate of the end-effector (m)

$\theta_1$ : the angular position of the joint 1 (rad)

$\theta_2$ : the angular position of the joint 2 (rad)

$\theta_3$ : the angular position of the joint 3 (rad)

$\theta_4$ : the angular position of the joint 4 (rad)

$\dot{\theta}_1$ : the angular velocity of the joint 1 ( $\frac{\text{rad}}{\text{s}}$ )

$\dot{\theta}_2$ : the angular velocity of the joint 2 ( $\frac{\text{rad}}{\text{s}}$ )

$\dot{\theta}_3$ : the angular velocity of the joint 3 ( $\frac{\text{rad}}{\text{s}}$ )

$\dot{\theta}_4$ : the angular velocity of the joint 4 ( $\frac{\text{rad}}{\text{s}}$ )

$\ddot{\theta}_1$ : the angular acceleration of the joint 1 ( $\frac{\text{rad}}{\text{s}^2}$ )

$\ddot{\theta}_2$ : the angular acceleration of the joint 2 ( $\frac{\text{rad}}{\text{s}^2}$ )

$\ddot{\theta}_3$ : the angular acceleration of the joint 3 ( $\frac{\text{rad}}{\text{s}^2}$ )

$\ddot{\theta}_4$ : the angular acceleration of the joint 4 ( $\frac{\text{rad}}{\text{s}^2}$ )

$i$ : gear ratio

$$\beta = \arccos\left(\frac{AC}{2 * l_2}\right) \quad (7)$$

$$\theta_3 = \alpha + \beta \quad (8)$$

$$\theta_2 = 180^\circ - (\beta - \alpha) \quad (9)$$

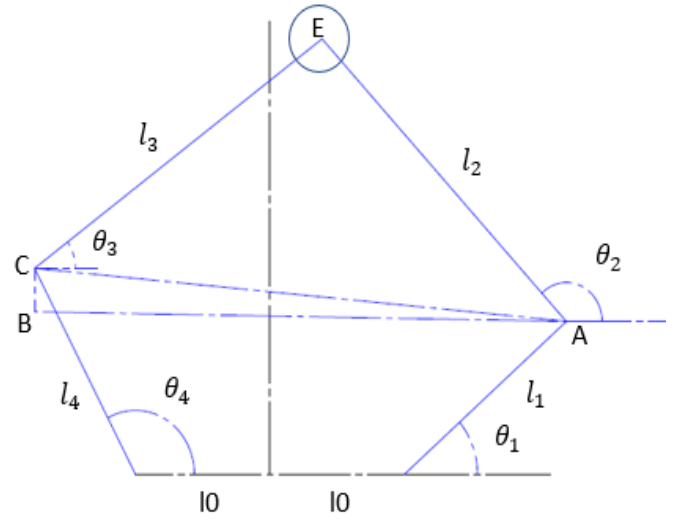


Figure 1. Kinematics analysis of the mechanism

## 2. METHODOLOGY

### 2.1 Kinematics

Kinematics can be defined as the motion study of objects regardless of the impact of masses and moments of inertia on the system components [6]. For analyzing the forward kinematics of the manipulator system, the relationships between the active links' angles ( $\theta_1$  and  $\theta_4$ ) and passive links' angles ( $\theta_2$  and  $\theta_3$ ) must be determined. The position vector of the end effector  $P_0^E$  allows determining the coordinates of the end effector for any given angles as clarified in the vectors shown in Eqs. (1) and (2). These relations are identified based on basic trigonometry and that can be shown with the help of Figure 1.

$$P_0^E = \begin{bmatrix} l_0 + l_1 \cos(\theta_1) + l_2 \cos(\theta_2) \\ l_1 \sin(\theta_1) + l_2 \sin(\theta_2) \\ 0 \end{bmatrix} \quad (1)$$

$$P_0^E = \begin{bmatrix} l_0 + l_4 \cos(\theta_4) + l_3 \cos(\theta_3) \\ l_4 \sin(\theta_4) + l_3 \sin(\theta_3) \\ 0 \end{bmatrix} \quad (2)$$

The Eqs. (3)-(9) help determining the relations between the angles:

$$AB = 2l_0 + \cos(\theta_4) * l_4 + \cos(\theta_1) * l_1 \quad (3)$$

$$BC = l_4 * \sin(\theta_4) - (l_1 \sin(\theta_1)) \quad (4)$$

$$AC = \sqrt{AB^2 + BC^2} \quad (5)$$

$$\alpha = \arctan\left(\frac{BC}{AB}\right) \quad (6)$$

#### Example:

Let's consider a simple planar 2-link robotic arm where the length of both links is 1 unit. The forward kinematics equations for this system can be represented as:

$$\begin{aligned} x &= \cos(\theta_1) + \cos(\theta_1 + \theta_2) \\ y &= \sin(\theta_1) + \sin(\theta_1 + \theta_2) \end{aligned}$$

Now, let's evaluate the end effector position ( $x, y$ ) for different common angles. Assume the following angles:

$$\begin{aligned} \theta_1 &= 30^\circ \\ \theta_2 &= 45^\circ \end{aligned}$$

Plugging these values into the equations, we get:

$$\begin{aligned} x &= \cos(30) + \cos(30+45) = 0.866 + 0.383 \approx 1.249 \\ y &= \sin(30) + \sin(30+45) = 0.5 + 0.574 \approx 1.074 \end{aligned}$$

Therefore, for the angles  $\theta_1=30^\circ$  and  $\theta_2=45^\circ$ , the end effector position is approximately (1.249, 1.074) units.

You can repeat this process by changing the values of  $\theta_1$  and  $\theta_2$  to demonstrate how the end effector coordinates change with different angles. If you have specific equations or parameters you'd like to work with, feel free to share them so we can provide a more tailored example.

### 2.2 Inverse kinematics

Inverse kinematics revolves around finding the required generalized coordinates (either displacements, angles, or both) for attaining the desired end effector coordinates of the manipulator [7]. For a given end effector's coordinates ( $x, y$ ) in the manipulator, the active links' angles must be determined. Figure 2 clarifies the relationship between the active link angles and the end effector coordinates.

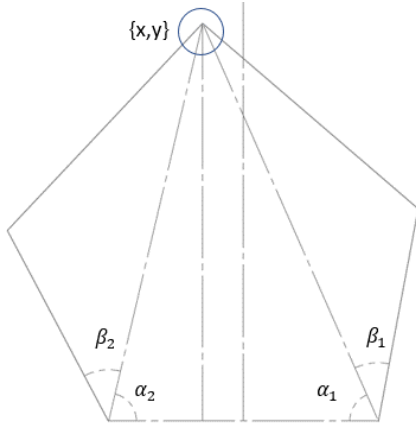


**Figure 2.** Inverse kinematics of the manipulator

The Eqs. (10)-(15) express the inverse kinematics formulas of the mechanism. By using these equations, any coordinates of the end effector are achievable based on the correct calculation of the corresponding active links' angles.

$$\alpha_1 = \arctan\left(\frac{y}{10-x}\right) \quad (10)$$

$$\beta_1 = \frac{\arccos(l_2^2 - (l_1^2 + x^2 + y^2))}{-2l_1\sqrt{x^2 + y^2}} \quad (11)$$

$$\theta_1 = (\pi - \text{real}(\alpha_1 + \beta_1)) * \frac{180}{\pi} \quad (12)$$

$$\alpha_2 = \arctan\left(\frac{y}{10+x}\right) \quad (13)$$

$$\beta_2 = \frac{\arccos(l_3^2 - (l_4^2 + x^2 + y^2))}{-2l_4\sqrt{x^2 + y^2}} \quad (14)$$

$$\theta_2 = (\text{real}(\alpha_1 + \beta_1)) * \frac{180}{\pi} \quad (15)$$

Example:

Let's consider these equations and work through a numerical example to demonstrate how we can compute the active link angles  $\theta_1$  and  $\theta_2$  for a given end effector coordinates  $(x, y)$ . Given:

- $l_1=5$  units
- $l_2=7$  units
- $l_3=6$  units
- $x=3$  units
- $y=4$  units

Using Eqs. (10)-(15), we can calculate the active link angles  $\theta_1$  and  $\theta_2$ :

$$\alpha_1 = \arctan(y / (10 - x)) \approx \arctan(4 / (10 - 3)) \approx \arctan(4 / 7) \approx 29.74^\circ$$

$$\beta_1 = \arccos((72 - (25 + 9)) / (-2 \times 5 \times \sqrt{(3^2 + 4^2)})) \approx \arccos(38 / (-10 \times 5)) \approx \arccos(-0.76) \approx 141.04^\circ$$

$$\theta_1 = (\pi - (29.74 + 141.04)) \times 180 / \pi \approx (\pi - 170.78) \times 180 / \pi \approx 97.83^\circ$$

$$\alpha_2 = \arctan(y / (10 + x)) \approx \arctan(4 / (10 + 3)) \approx \arctan(4 / 13) \approx 16.70^\circ$$

$$\beta_2 = \arccos((36 - (36 + 9)) / (-2 \times 6 \times \sqrt{(3^2 + 4^2)})) \approx$$

$$\arccos(-9 / (-12 \times 5)) \approx \arccos(0.15) \approx 81.84^\circ$$

$$\theta_2 = (16.70 + 81.84) \times 180 / \pi \approx 98.54^\circ$$

Therefore, for the given end effector coordinates  $x=3$  units,  $y=4$  units, the corresponding active link angles are approximately:  $\theta_1 \approx 97.83^\circ$ ,  $\theta_2 \approx 98.54^\circ$ .

By plugging these angles back into the forward kinematics equations, you should be able to validate that they indeed produce the desired end effector position of (3, 4) units.

### 2.3 Dynamic

Mathematical models of robot dynamics describe the motion of objects while external forces, torques, or both act on the robot system. Robotic dynamic equations are used in robotic control systems in order to achieve the desired behavior of the robot, which is to track and adhere to the planned path. Further, the system dynamics represent the equation of motion EOM of the system [8].

For many applications of robotic systems, there is a need to find the dynamic study of multi-body robots as follows:

The positions of the centers of mass of each link are expressed as in Eqs. (16)-(19):

$$\vec{r}_{c1} = \begin{bmatrix} l_0 + l_{c1} \cos(\theta_1) \\ l_{c1} \sin(\theta_1) \\ 0 \end{bmatrix} \quad (16)$$

$$\vec{r}_{c2} = \begin{bmatrix} l_0 + l_1 \cos(\theta_1) + l_{c2} \cos(\theta_2) \\ l_1 \sin(\theta_1) + l_{c2} \sin(\theta_2) \\ 0 \end{bmatrix} \quad (17)$$

$$\vec{r}_{c3} = \begin{bmatrix} l_0 + l_4 \cos(\theta_4) + l_{c3} \cos(\theta_3) \\ l_4 \sin(\theta_4) + l_{c3} \sin(\theta_3) \\ 0 \end{bmatrix} \quad (18)$$

$$\vec{r}_{c4} = \begin{bmatrix} l_0 + l_{c4} \cos(\theta_4) \\ l_{c4} \sin(\theta_4) \\ 0 \end{bmatrix} \quad (19)$$

Therefore, the velocities of the centers of mass of each link can be calculated as in Eq. (20):

$$\vec{V}_{c1} = \frac{d(r_{c1})}{dt}, \vec{V}_{c2} = \frac{d(r_{c2})}{dt},$$

$$\vec{V}_{c3} = \frac{d(r_{c3})}{dt}, \vec{V}_{c4} = \frac{d(r_{c4})}{dt} \quad (20)$$

Then:

$$V_1 = \begin{bmatrix} -l_{c1} \sin(\theta_1) * \theta_1' \\ l_{c1} \cos(\theta_1) * \theta_1' \\ 0 \end{bmatrix} \quad (21)$$

$$V_2 = \begin{bmatrix} -l_1 \sin(\theta_1) * \theta_1' - l_{c2} \sin(\theta_2) * \theta_2' \\ l_1 \cos(\theta_1) * \theta_1' + l_{c2} \cos(\theta_2) * \theta_2' \\ 0 \end{bmatrix} \quad (22)$$

$$V_3 = \begin{bmatrix} -l_4 \sin(\theta_4) * \theta_4' - l_{c3} \sin(\theta_3) * \theta_3' \\ l_4 \cos(\theta_4) * \theta_4' + l_{c3} \cos(\theta_3) * \theta_3' \\ 0 \end{bmatrix} \quad (23)$$

$$V_4 = \begin{bmatrix} -l_{c4} \sin(\theta_4) * \theta_4' \\ l_{c4} \cos(\theta_4) * \theta_4' \\ 0 \end{bmatrix} \quad (24)$$

In the subsequent stage, the kinetic and potential energies of the system are determined. The kinetic energy of the mechanism is calculated as in Eq. (25):

$$E_{total} = E_{k1} + E_{k2} + E_{k3} + E_{k4} \quad (25)$$

However, the system motion is bound with the XY planar, which implies no motion along the Z axis. Hence, the potential energy of the system is considered zero:

$$E_{P_{1,2,3,4}} = 0 \Leftrightarrow (Z = 0) \quad (26)$$

Nevertheless, the kinetic energies of the mechanism are the summation of the kinetic energy and rotational energy as in Eqs. (27)-(31):

$$E_k = E_{K_{linear}} + E_{K_{rotational}} \quad (27)$$

$$\begin{aligned} E_{k1} &= 0.5 m_1 (V_{c1}^T \cdot V_{c1}) + 0.5 I_{\frac{1}{c}} (w_1^T \cdot w_1) \\ &= 0.5 m_1 \|V_{c1}\|^2 + 0.5 I_{\frac{1}{c}} \|w_1\|^2 \end{aligned} \quad (28)$$

$$E_{k1} = 0.5 m_1 (l_{c1}^2) \dot{\theta}_1^2 + 0.5 I_{\frac{1}{c}} \dot{\theta}_1^2$$

Similarly:

$$E_{k2} = \frac{1}{2} m_2 V_{c2}^T V_{c2} + \frac{1}{2} I_{\frac{2}{c}} \dot{\theta}_2^2 \quad (29)$$

$$\begin{aligned} E_{k3} &= \frac{1}{2} I_{\frac{3}{c}} \dot{\theta}_3^2 + \frac{1}{2} m_3 (l_{c4}^2 \dot{\theta}_4^2 + l_{3c}^2 \dot{\theta}_3^2 \\ &\quad + l_4 l_{3c} \dot{\theta}_3 \dot{\theta}_4 \cos(\theta_4 - \theta_3)) \end{aligned} \quad (30)$$

$$E_{k4} = \frac{1}{2} (I_4 + l_{c4}^2 m_4) \dot{\theta}_4^2 \quad (31)$$

Now the Lagrangian is identified as in Eq. (32):

$$L = E_{K_{total}} - E_{P_{total}} = E_{k1} + E_{k2} + E_{k3} + E_{k4} \quad (32)$$

Through Lagrangian equations the torques applied to each joint can be determined as in Eqs. (33) and (34):

$$\tau_1 = \frac{d}{dt} \left( \frac{dL}{d\dot{\theta}_1} \right) - \frac{dL}{d\theta_1}, \quad \tau_2 = \frac{d}{dt} \left( \frac{dL}{d\dot{\theta}_2} \right) - \frac{dL}{d\theta_2} \quad (33)$$

$$\tau_3 = \frac{d}{dt} \left( \frac{dL}{d\dot{\theta}_3} \right) - \frac{dL}{d\theta_3}, \quad \tau_4 = \frac{d}{dt} \left( \frac{dL}{d\dot{\theta}_4} \right) - \frac{dL}{d\theta_4} \quad (34)$$

#### Example:

To demonstrate the applicability of the equations in determining the coordinates of the final effect, let's consider a numerical example with the following parameters:

$$\begin{aligned} l_0 &= 2 \text{ units} \\ l_{c1} &= 1 \text{ unit} \\ l_{c2} &= 1.5 \text{ units} \\ l_{c3} &= 1.8 \text{ units} \\ l_{c4} &= 1.2 \text{ units} \\ m_1 &= 3 \text{ kg} \\ m_2 &= 2 \text{ kg} \\ m_3 &= 2.5 \text{ kg} \\ m_4 &= 1.5 \text{ kg} \end{aligned}$$

$$\begin{aligned} I_{1/c} &= 0.5 \text{ kg.m}^2 \\ I_{2/c} &= 0.7 \text{ kg.m}^2 \\ I_{3/c} &= 1 \text{ kg.m}^2 \\ I_{4/c} &= 0.4 \text{ kg.m}^2 \\ \theta_1 &= 30^\circ \\ \theta_2 &= 45^\circ \\ \theta_3 &= 60^\circ \\ \theta_4 &= 15^\circ \end{aligned}$$

Using the provided equations, we can calculate the kinetic energies  $E_{k1}$ ,  $E_{k2}$ ,  $E_{k3}$ ,  $E_{k4}$ , and the Lagrangian L, and then determine the torques  $\tau_1$ ,  $\tau_2$ ,  $\tau_3$ , and  $\tau_4$  applied to each joint.

After these calculations, we can validate the results and see how they contribute to understanding the dynamics of the multi-body robot system with the given joint angles. It's a great way to showcase the practical application of these complex equations in robotics.

## 2.4 Gearing devices

In general, electrical motors generate relatively small torques while spanning at elevated speeds [9]. ( $Power=torque \times angular \ velocity$ ). Consequently, it is necessary to employ adequate gearing for the electrical motors to make them capable of driving relatively large loads (that demand large torques) at decreased velocities. For instance, robot links are typically moved at reduced speeds, less than 60 rpm, while it is required to provide maximum torques varying from a few newton meters to a couple hundred newton meters [10]. A load is driven by a motor through a gear train, which consists of two gears coupled together. The primary gear has  $N_1$  teeth and the secondary gear contains  $N_2$  teeth (In our proposed project scheme  $N_1=... N_2=...$ ).  $\theta_1$  and  $\theta_2$  are the angular displacements of the shafts 1 and 2. The viscous friction and the moment of inertia of gear 1 are denoted by  $B_1$  and  $J_1$  respectively, whilst  $B_2$  and  $J_2$  represent the viscous friction and the moment of inertia of gear 2 and load respectively.  $T_M$  represents the developed torque by the motor, and the torque of disturbance on the load is denoted by  $T_w$ .

Figure 3 shows the free-body diagram of the drive-train system. Since,  $T_{12}$  is the applied torque on gear 1 from the gear 2, and the transmitted torque to gear 2 from gear 1. The equivalent Eqs. (35) and (36) are for this system [11]:

$$J_1 \ddot{\theta}_1 + B_1 \dot{\theta}_1 + T_{21} = T_M \quad (35)$$

For the load shaft,

$$J_2 \ddot{\theta}_2 + B_2 \dot{\theta}_2 + T_w = T_{21} \quad (36)$$

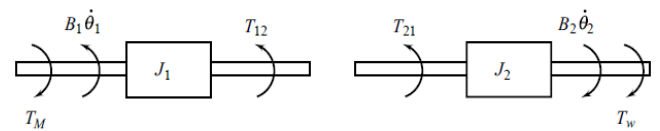


Figure 3. Free body diagrams of the drive train system

The following relationship:  $\theta_2 = \left( \frac{N_1}{N_2} \right) \theta_1$  expresses the idealized characteristics of the gear train. However, in real applications, a certain quantity of free play “backlash” between coupled gears occurs. Assuming  $r_1$  is the radius of gear 1 and the radius of gear 2 is  $r_2$ . Knowing that the linear velocity transmitted from gear 1 to gear 2 is the same along

the coupled gears  $\theta_1 r_1 = \theta_2 r_2$ . The Eq. (37) represents the dynamics of the drive-train system:

$$\frac{T_{12}}{T_{21}} = \frac{N_1}{N_2} = \frac{\theta_2}{\theta_1} \quad (37)$$

By applying the differentiation to Eq. (37) twice, we obtain [12]:

$$\frac{\ddot{\theta}_2}{\dot{\theta}_1} = \frac{\dot{\theta}_2}{\dot{\theta}_1} = \frac{N_1}{N_2} \quad (38)$$

Based on Eqs. (37) and (38), it is observed from  $(N_1/N_2) < 1$  that the gear train gives speed reduction and torque magnification by selecting  $\frac{N_1}{N_2}$  properly. By rearranging and simplifying the Eqs. (35) and (36) with the assistance of Eq. (38). It is obtained:

$$J_1 \ddot{\theta}_1 + B_1 \dot{\theta}_1 + \frac{N_1}{N_2} (J_2 \ddot{\theta}_2 + B_2 \dot{\theta}_1 + T_w) = T_M \quad (39)$$

With the help of Eq. (38)  $\theta_2$  is eliminated from Eq. (39), and it yields:

$$\left[ J_1 + \left( \frac{N_1}{N_2} \right)^2 J_2 \right] \ddot{\theta}_1 + \left[ B_1 + \left( \frac{N_1}{N_2} \right)^2 B_2 \right] \dot{\theta}_1 + \frac{N_1}{N_2} T_w = T_M \quad (40)$$

The Eq. (40) can be expressed alternatively as follows:

$$J_{eq} \ddot{\theta}_1 + B_{eq} \dot{\theta}_1 + T_{weq} = T_M \quad (41)$$

#### Example:

Understanding the dynamics of a drive-train system with gears and torque transmission is crucial for designing efficient robotic systems with motors. The equations provided describe the relationships between angular displacements, torques, moments of inertia, and friction in the system.

To demonstrate the applicability of the equations in determining the coordinates of the final effect for different common angles, we can consider a numerical example with the following parameters:

$$J_1 = 0.8 \text{ kg.m}^2$$

$$B_1 = 0.1 \text{ N.m.s/rad}$$

$$J_2 = 0.5 \text{ kg.m}^2$$

$$B_2 = 0.2 \text{ N.m.s/rad}$$

$$N_1 = 20 \text{ (number of teeth on gear 1)}$$

$$N_2 = 40 \text{ (number of teeth on gear 2)}$$

$$T_M = 5 \text{ N.m (torque developed by the motor)}$$

$$T_w = 1 \text{ N.m (external torque disturbance on the load)}$$

Using the given Eqs. (35)-(41) and the provided parameters, we can solve for the angular displacement  $\theta_1$ , angular acceleration  $\ddot{\theta}_1$ , and other variables in the system to understand how the system behaves under these conditions. By substituting the values into the equations and performing the calculations, we can observe how the motor torque, gear ratios, inertia, and friction influence the motion of the system.

After solving the equations numerically, we can analyze the results to gain insights into how the drive-train system responds to different angles, torques, and gear configurations.

It's a practical way to illustrate the theoretical concepts in action and showcase the importance of these dynamics in designing efficient robotic systems.

## 3. RESULTS AND DISCUSSION

The positioning accuracy of the end-effector of the 2DOF five-bar robot was investigated in the study. This was accomplished by modeling a variety of goal locations as well as the actual ones attained by the robot. The results show that the positioning accuracy changes with distance from the base and end-effector orientation. When the end-effector is closer to the base, the accuracy improves.

### 3.1 Trajectory planning

In the first stage, a set of points expressed as coordinates  $(x, y, z)$  describe the end-effector's route in the three-dimensional setup. This path can be used in the inverse kinematics equations to compute the required path for each robot joint to obtain the desired end-effector coordinates. It can be represented as a function of the spatial coordinates  $(x, y, z)$ . But in order to make these pathways more realistic, temporal and spatial elements must be included. Trajectory planning, which uses trajectory as a function of  $(x, y, z, t)$  to generate reference signals for the robot's control system, depends on this conversion from path to trajectory.

When transferring the robotic arm and end-effector from an initial position to a desired position, a number of factors must be taken into account:

- (1) Remaining within the joint's maximum generalized coordinate values is important to maintain motion limitations.
- (2) Making sure the trajectory doesn't cause excessive vibrations that could cause mechanical problems.

In a quantitative analysis, the links' positions are differentiated over time to determine the velocity as a function of time, and the velocity is further differentiated to determine the acceleration as a function of time. The active joint angles needed to move the robot's end effector from its initial position to the intended position are found using an inverse kinematics analysis. This data (see Figure 4) help determine the torque that the motors must produce in order to enable the movement.

For example, using computational tools such as Matlab, appropriate angles for the active joints ( $\theta_1=84.4595^\circ$  and  $\theta_4=83.0809^\circ$ ) are discovered in order to move the end effector from position A (0 cm, 25 cm) to position B (4 cm, 29 cm). Next, given a total motion period of 5 seconds, the movement of the end effector over time to reach the desired position is assessed based on trajectory planning equations, usually analyzed using software tools like Matlab (see Figure 5).

A statistical study on the trajectories or joint coordinates could be carried out to provide quantitative support for the conclusions. This could entail calculating the standard deviation of joint angles, the mean departure from the intended path, or comparing the actual and expected values of joint angles. Furthermore, examining the acceleration profiles and contrasting them with predetermined boundaries may offer valuable perspectives on system functionality and substantiate the trajectory planning methodology. By doing statistical analysis, the study's credibility and relevance in robotic system design and control would be further strengthened, providing a more solid validation of the findings.

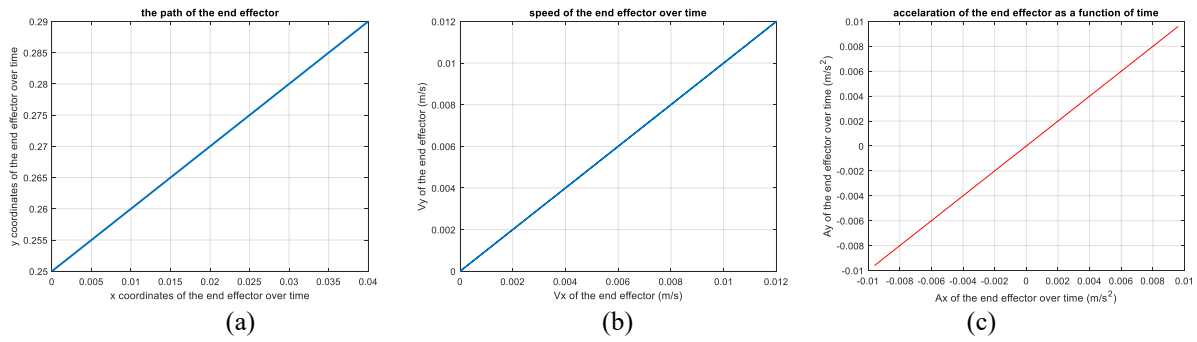


**Figure 4.** Position (a), speed (b) and acceleration (c) of the end-effector over time

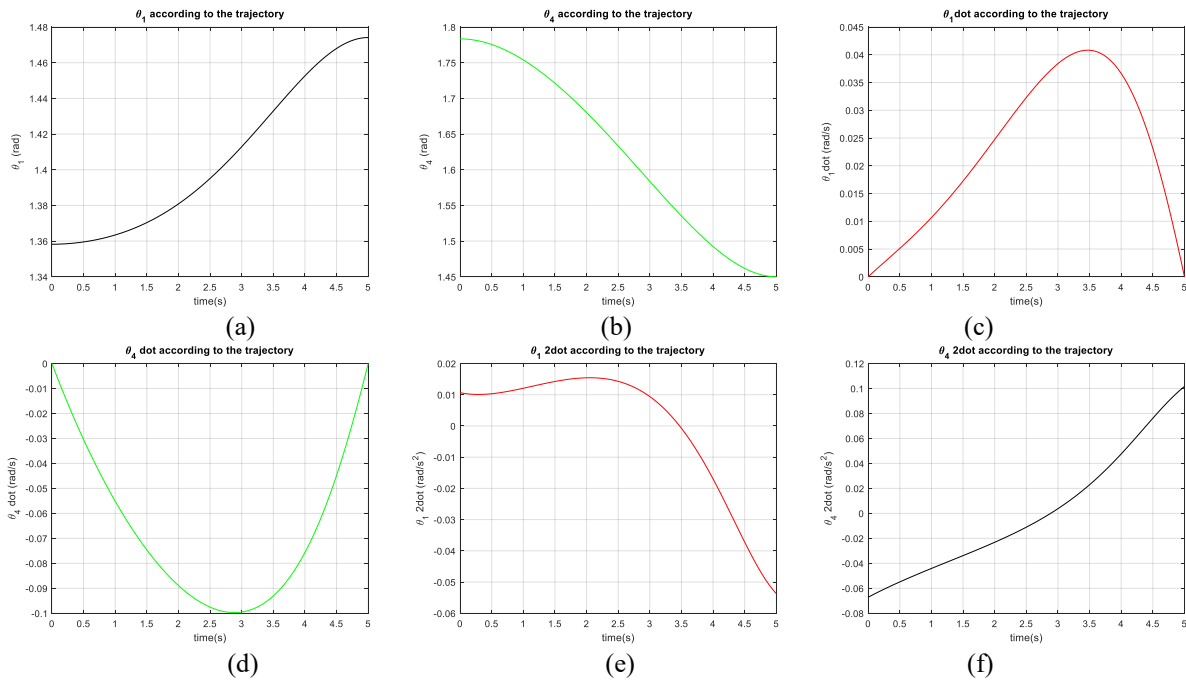


**Figure 5.**  $\theta_1$ (a),  $\theta_4$ (b),  $\dot{\theta}_1$ (c),  $\dot{\theta}_4$ (d),  $\ddot{\theta}_1$ (e), and  $\ddot{\theta}_4$ (f) according to the trajectory

The motors are expected to generate a velocity output four times higher than the stipulated velocity in order to meet the system requirements. The gearing arrangement in use, which multiplies the motor speed by four, makes this necessary.

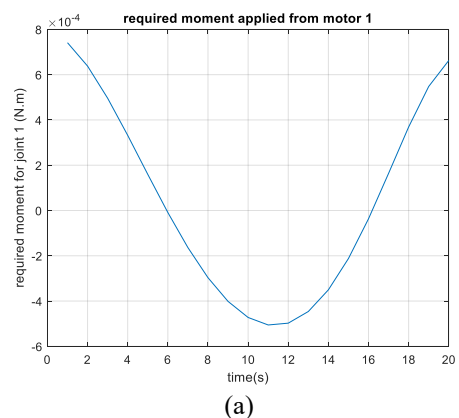
Then, the generalized coordinates of the active joints are integrated into the robot's dynamic equations to calculate the torque that the motors must produce in order to carry out the intended trajectory. The gear ratio—a term used to describe how much the gearing system increases the applied torques from the motors—is four.

After this investigation, Figure 6(a) shows the calculated torque required from motor 1 using computational tools such as Matlab. Similarly, Figure 6(b) shows the torque needed from the second motor in order to drive joint 4. The torque demands made on the motors during the motion execution process are made clear by these graphic representations.

The torque profiles of the motors could be assessed statistically in order to offer more robust quantitative support. Metrics like peak torque values, torque fluctuations, or a comparison between theoretical calculations and real torque requirements could be used in this. Furthermore, statistical metrics such as variance in torque demands or examination of torque distribution across various joints may provide more comprehensive understanding of the system's functioning and

support the torque estimates obtained from the dynamics equations.

Through the implementation of quantitative analyses, researchers are able to get a more thorough comprehension of the torque requirements for the motor and determine whether the amplification of the gearing system is in line with the anticipated torque demands. These statistical analyses strengthen the conclusions' robustness and support a more evidence-based strategy for maximizing the effectiveness and performance of the robotic system.



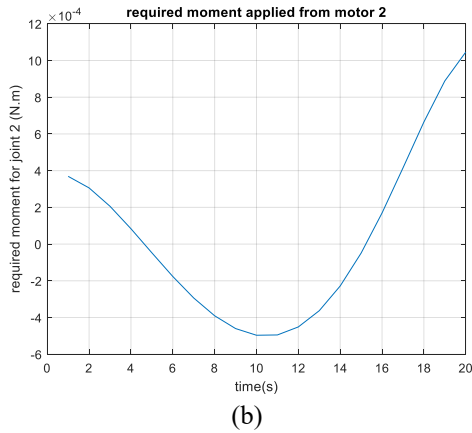


**Figure 6.** Required torque applied from motor 1 (a) and motor 2 (b)

### 3.2 Actuators and control systems

The role of the actuators is to move and reposition a joint or arm. The role of the feedback control systems is to ensure that the planned trajectory is satisfactorily achieved. In general, a control system whose role is to control the position of a system and track its movements is called a servomechanism [13]. Figure 7 shows a simplified depiction of a robot control system:

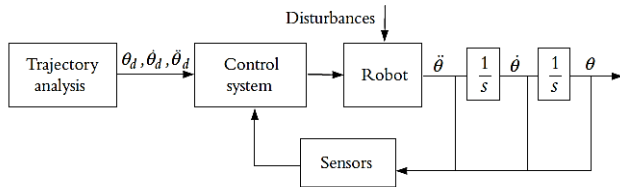


**Figure 7.** Simplified diagram of robot control system

As previously explained, the joint values and variables (position, velocity, acceleration, forces, and torques) are calculated based on kinematic, dynamic, and trajectory analysis. These values and variables are sent to the controller so that the controller, in return, applies stimulus (operating) signals to actuators (e.g., motors) to move and operate the joints to their desired destination in a controlled manner. Sensors measure the outputs and send signals back to the controller, which in turn controls the operational signals. For a multi-joint robot (MIMO system), in most cases, the robot is controlled by controlling each joint independently from the rest of the joints in a way called "controlling each joint separately" and considering each joint as one with a single input and a single output. The effects of overlapping connections by other joints are often treated as noise and handled by the controller. Moreover, robot dynamic equations have highly non-linear behavior, which in turn requires more complex control systems [14].

On the other hand, actuators are the muscles of the robot. Since the joints and connections are the skeleton of the robot, the actuators are the muscles that move or rotate the connections to change the structure of the robot. The actuators must have sufficient capacity to speed up or lighten the joints and to carry loads effectively. There are many types of triggers, including electric motors, servomotors, stepper motors, hydraulic actuators, pneumatic actuators, and novelty actuators [15].

Electric motors, especially servomotors, are the most common actuators in robotics applications. Hydraulic actuators were very popular in the past, but nowadays they are less used, except for large applications. Pneumatic actuators are used in pneumatic robots that have a half degree of freedom and on/off joints. The novel actuators, which may include direct drive actuators, cable-muscle actuators, and others, are often used in research centers and for development objectives.

The differences between the reference signals (represented by required  $\theta_1$  and  $\theta_4$  based on planned trajectory) and the robot joints' response (dynamics) are calculated, and that expresses the error in the closed-loop system.

The dynamic responses of the manipulator and the active joints are depicted in Figure 8 (a) and (b).

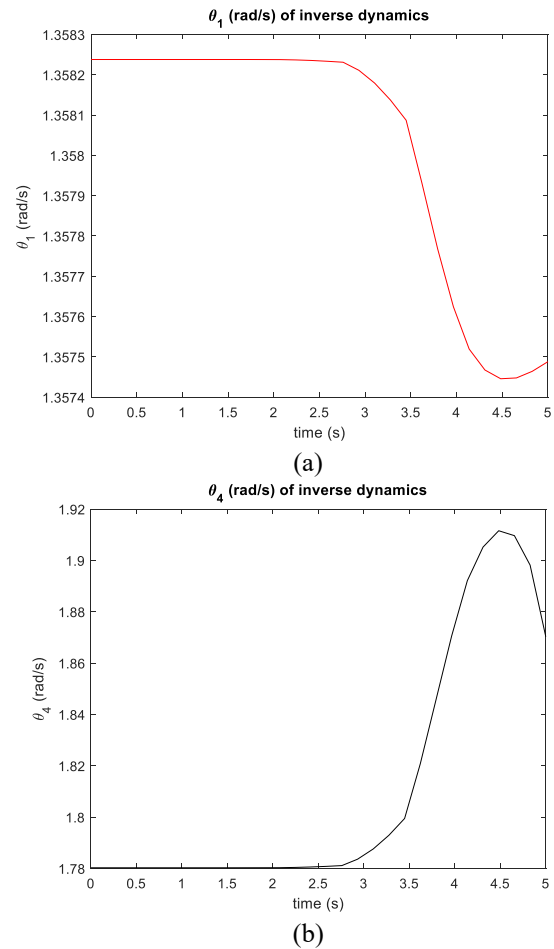


**Figure 8.** The dynamic response of the active joint 1 (a) and 2 (b)

Error correction that resulted from the differences between the reference signals and dynamics response is conducted through the PID controller in the SIMULINK environment, as illustrated in Figure 9.

For a robotic arm or joint to move and position more easily, actuators are essential. However, in order to guarantee that planned trajectories are executed accurately, feedback control systems are necessary. A servomechanism is a control system used in robotics that is mainly responsible for tracking movement and adjusting system position. Kinematic, dynamic, and trajectory analyses provide the means by which the system can regulate joint values such as position, velocity, acceleration, forces, and torques.

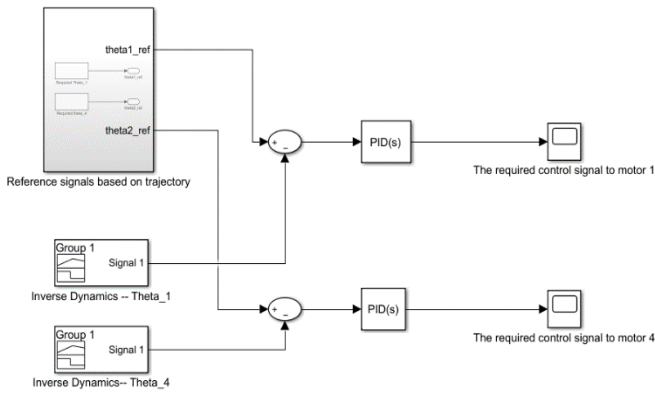


**Figure 9.** Correction of the error caused by the differences between the reference signal and the dynamical response by the controllers

Every joint of a multi-joint robot is usually controlled separately, as if it were a single input-single-output system. In order to preserve accuracy and stability, the controller often handles the joint interaction effects as disturbances. Robust control systems are necessary for efficient operation due to the non-linear nature of robot dynamic equations.

Actuators are the "muscles" of the robot; they move or rotate connections to change the structure of the robot. To drive movements, support loads, and accelerate joints, they must have sufficient power. Actuators come in a variety of forms: electric motors (particularly servomotors, which are extensively utilized in robotics) to hydraulic and pneumatic actuators, as well as newer choices such cable-muscle and direct drive actuators.

Robotic systems typically use certain control methods, such Proportional-Integral-Derivative (PID) control, to manage performance. PID controllers have benefits in terms of robustness, simplicity, and tuning ease. On the other hand, their ability to manage intricate, non-linear dynamics may be limited, and they may not perform well in situations when exact trajectory tracking or disturbance rejection are necessary.

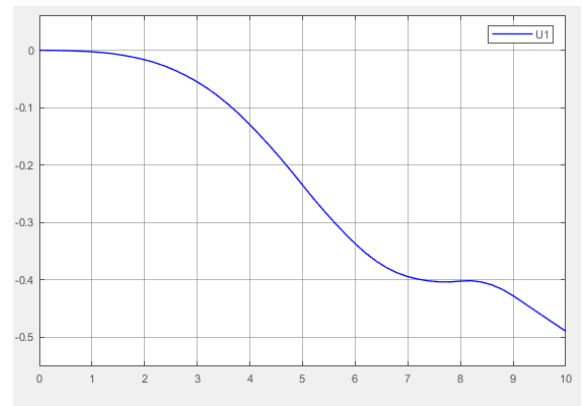
The controller creates signals during the control process based on the variations between reference signals (such as intended joint angles) and the real joint responses. The goal of this feedback loop is to reduce errors and guarantee precise motion along predetermined paths. Actuators' activities are influenced by control signals, which in turn affect the end-effector's mobility and location within the operational space.

Accurate and smooth trajectory tracking of end-effector movement depends critically on the timing and precision of the control signal. PID control algorithms are essential for fine-tuning the actuators' actions to efficiently perform desired movements. It is crucial to comprehend how actuator dynamics, control algorithms, and end-effector behavior interact in order to maximize robotic system performance and improve job execution capabilities.

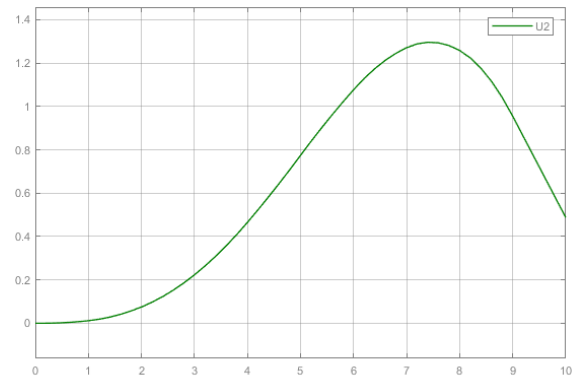
The control signals that are generated by the controllers are needed to move the end-effector to the desired coordinates, as shown in Figure 10 (a) and (b).

The study investigated the end effector positioning accuracy of a five-bar robot with 2 degrees of freedom (DOF), highlighting how accuracy varies with distance from the base and direction of the end effector. The research involved modeling the locations of different targets and comparing them to the actual locations achieved by the robot. It is worth noting that it was noted that the positioning accuracy improves

as the end effector approaches the base.



(a)



(b)

**Figure 10.** The control signal  $U_1$  which affect the motor 1 (a) and the control signal  $U_2$  which affect the motor 2 (b)

With regard to path planning, the study emphasized the importance of determining the path of the final effector in a three-dimensional setting as a function of the coordinate axes ( $x, y, z$ ). The path required for each joint of the robot was also determined to reach the required final effector coordinates, as moving from paths to paths required taking into account variables. Temporal and spatial, and by incorporating this path function into the inverse kinematics equations, which led to enhancing the realism of the planned paths.

The need to ensure that the robotic arm moves smoothly from its initial position to the desired location was also highlighted, as this includes factors such as staying within the limits of joint motion, avoiding excessive vibrations that may compromise mechanical integrity, and achieving the desired speed outputs by taking into account the gear system.

Furthermore, the discussion touched on the role of operators in facilitating joint movement and the importance of feedback control systems in monitoring and achieving the desired path. The study emphasized the importance of the servo mechanism in controlling the system's position and tracking its movements effectively.

The use of actuators, such as electric motors and servo motors, has been emphasized as essential for executing intended movements, and the use of sophisticated control systems, such as proportional and integral derivative (PID) controllers, has been shown to be instrumental in correcting errors between the planned path and the actual dynamic response.

To understand the implications of the findings on improving robotic system accuracy and investigating possible



applications, a thorough analysis and interpretation of the data are required. Some of the areas that could benefit from further research include optimizing trajectory planning algorithms, improving control strategies for better system performance, and investigating novel actuator technologies for robotic applications. These directions could lead to advancements in the design and operation of robotic systems.

In conclusion, research on the 2DOF five-bar robot's end-effector positioning precision has shed light on the complex dynamics of robotic systems. The results highlight the importance of end-effector orientation and distance from the base in determining positioning accuracy, highlighting the requirement for accuracy in trajectory planning and control systems.

The results show improvements in our knowledge of end-effector movement and control processes in robotic systems when compared to previous research. The inquiry has clarified the significance of trajectory planning, joint dynamics, and feedback control systems in obtaining precise and effective movements. The study enhances the reliability and performance of robotic systems by highlighting the significance of actuators and control algorithms.

It is imperative to recognize the possible constraints of the research, though. In various contexts, the robustness of control algorithms may be affected by variations in real-world conditions, environmental influences, and unforeseen disturbances. In order to guarantee optimal performance and dependability in real-world applications, more investigation is necessary into the adaptability of control techniques in dynamic and uncertain situations.

In order to improve the agility and efficacy of robotic systems, future research could concentrate on improving trajectory planning algorithms, improving control techniques for a range of operational circumstances, and investigating novel actuator technologies. We can keep advancing the design and application of complex robotic platforms with greater precision and adaptability by tackling these issues and utilizing developments in control theory and robotics.

#### 4. CONCLUSIONS

From the above, we find that we have provided a comprehensive overview of the study on the closed-chain parallel robot system, identifying various aspects such as kinematics, dynamics, path planning, motor control systems, and gear mechanisms to enhance accuracy and efficiency. The Methodology section details the step-by-step process involved in analyzing and improving an automated system.

We also find that the results and discussion section highlights the results related to the accuracy of determining the position of the final effector, path planning, engine torque analysis, and the role of motors and control systems, as these results highlight the importance of precise control and efficient movement in robotic systems, especially in industrial applications where it is Accuracy and reliability are crucial.

The equations and practical application examples presented by the research also review theoretical concepts in the field of robotics, demonstrating how different parameters and dynamics affect the behavior of the robotic system. The Matlab-Simulink integration of path planning and control algorithms adds a practical dimension to the study, enabling effective control and optimization of the automated system.

In conclusion of the summary, we can emphasize the importance of this study in developing the field of closed-chain parallel robots, improving manufacturing processes, and improving industrial automation. We can also mention the potential implications of the research results in real-world applications and the development of advanced control algorithms to enhance accuracy and efficiency.

Ultimately, we expect that this study covers the fundamental aspects of automated system analysis and optimization, and the integration of mathematical models, simulations, and practical examples adds depth to the research, and effectively presents the methodology and results.

#### REFERENCES

- [1] Nzue, R.M.A., Brethé, J.F., Vasselín, E., Lefebvre, D., Comparison of serial and parallel robot repeatability based on different performance criteria. *Mechanism and Machine Theory*, 61: 136-155. <https://doi.org/10.1016/j.mechmachtheory.2012.10.004>
- [2] Gutierrez, M.N.C. Dimensional synthesis of 3RRR planar parallel robots for well-conditioned workspace. *IEEE Latin America Transactions*, 13(2): 409-415. <https://doi.org/10.1109/TLA.2015.7055557>
- [3] Murphy, M.A., Sunnerhagen, K.S., Johnels, B., Willén, C. (2006). Three-dimensional kinematic motion analysis of a daily activity drinking from a glass: A pilot study. *Journal of Neuroengineering and Rehabilitation*, 3: 1-11. <https://doi.org/10.1186/1743-0003-3-18>
- [4] Ivanovic, A., Car, M., Orsag, M., Bogdan, S. (2020). Exploiting null space in aerial manipulation through model-in-the-loop motion planning. In 2020 International Conference on Unmanned Aircraft Systems (ICUAS), Athens, Greece, pp. 686-693. <https://doi.org/10.1109/ICUAS48674.2020.9213914>
- [5] Schoenenberger, L., Schmid, A., Tanase, R., Beck, M., & Schwaninger, M. (2021). Structural analysis of system dynamics models. *Simulation Modelling Practice and Theory*, 110: 102333. <https://doi.org/10.1016/j.simpat.2021.102333>
- [6] Li, S., Li, Y., Choi, W., Sarlioglu, B. (2016). High-speed electric machines: Challenges and design considerations. *IEEE Transactions on Transportation Electrification*, 2(1): 2-13. <https://doi.org/10.1109/TTE.2016.2523879>
- [7] Giberti, H., La Mura, F., Resmini, G., Parmeggiani, M. (2018). Fully mechatronical design of an hil system for floating devices. *Robotics*, 7(3): 39. <https://doi.org/10.3390/robotics7030039>
- [8] Cao, F., Jiang, H. (2021). Trajectory planning and tracking control of unmanned ground vehicle leading by motion virtual leader on expressway. *IET Intelligent Transport Systems*, 15(2): 187-199. <https://doi.org/10.1049/itr2.12013>
- [9] Badreddine, E.L., Houidi, A., Affi, Z., Romdhane, L. (2013). Application of multi-objective genetic algorithms to the mechatronic design of a four bar system with continuous and discrete variables. *Mechanism and Machine Theory*, 61: 68-83. <https://doi.org/10.1016/j.mechmachtheory.2012.11.002>
- [10] Cao, F., Liu, J. (2018). Optimal trajectory control for a two-link rigid-flexible manipulator with ODE-PDE model. *Optimal Control Applications and Methods*, 39(4): 1515-1529. <https://doi.org/10.1002/oca.2423>

- [11] Dixit, S., Fallah, S., Montanaro, U., Dianati, M., Stevens, A., Mccullough, F., Mouzakitis, A. (2018). Trajectory planning and tracking for autonomous overtaking: State-of-the-art and future prospects. *Annual Reviews in Control*, 45: 76-86. <https://doi.org/10.1016/j.arcontrol.2018.02.001>
- [12] Liu, G.F., Li, H.W. (2016). Design of stepper motor position control system based on DSP. In 2017 2nd International Conference on Machinery, Electronics and Control Simulation (MECS 2017), Taiyuan, China, pp. 207-211. <https://doi.org/10.2991/mecs-17.2017.38>
- [13] Iqbal, J., Ullah, M., Khan, S.G., Khelifa, B., Čuković, S. (2017). Nonlinear control systems-A brief overview of historical and recent advances. *Nonlinear Engineering*, 6(4): 301-312. <https://doi.org/10.1515/nleng-2016-0077>
- [14] Bobrow, J.E., Dubowsky, S., Gibson, J. S. (1985). Time-optimal control of robotic manipulators along specified paths. *The International Journal of Robotics Research*, 4(3): 3-17. <https://doi.org/10.1177/027836498500400301>
- [15] Wan, E.A., Van Der Merwe, R. (2000). The unscented Kalman filter for nonlinear estimation. In *Proceedings of the IEEE 2000 Adaptive Systems for Signal Processing, Communications, and Control Symposium (Cat. No. 00EX373)*, Lake Louise, AB, Canada, pp. 153-158. <https://doi.org/10.1109/ASSPCC.2000.882463>